Effect of Salt on the Formation of Alcohol−Dehydrogenease Monolayer: A Study by the Langmuir−Blodgett Technique

ARTICLE *in* THE JOURNAL OF PHYSICAL CHEMISTRY B · MAY 2009

Impact Factor: 3.3 · DOI: 10.1021/jp9001059 · Source: PubMed

4 AUTHORS, INCLUDING:

Prabir Pal
Indian Association for the Cultivation of Sci…
73 PUBLICATIONS **806** CITATIONS
SEE PROFILE

Mrityunjoy Mahato
North Eastern Hill University
21 PUBLICATIONS **270** CITATIONS
SEE PROFILE

THE JOURNAL OF PHYSICAL CHEMISTRY B

Article

Effect of Salt on the Formation of Alcohol-Dehydrogenease Monolayer: A Study by the Langmuir#Blodgett Technique

Tapanendu Kamilya, Prabir Pal, Mrityunjoy Mahato, and G. B. Talapatra

J. Phys. Chem. B, **2009**, 113 (15), 5128-5135• DOI: 10.1021/jp9001059 • Publication Date (Web): 25 March 2009

Effect of Salt on the Formation of Alcohol-Dehydrogenease Monolayer: A Study by the Langmuir−Blodgett Technique

Tapanendu Kamilya,[†,‡] Prabir Pal,[†] Mrityunjoy Mahato,[†] and G. B. Talapatra*[,†]

Department of Spectroscopy, Indian Association for the Cultivation of Science, Jadavpur, Kolkata-700 032, India, and Department of Physics, Narajole Raj College, Narajole, Paschim Medinipur −721 211, India

Received: January 6, 2009; Revised Manuscript Received: March 3, 2009

We report here the effect of salt (KCl) on the interfacial surface activity of yeast alcohol dehydogenease (ADH) at air/water interface using the Langmuir−Blodgett technique. Effect of salt content in the water subphase on ADH structure has been studied. The change of area/molecule, compressibility, rigidity, and unfolding of ADH are insignificant up to 10 mM KCl concentration. The significant changes are observed above 0.1 M KCl concentrations. Observations are explained in the context of DLVO theory. FTIR study of amide band together with AFM imaging of ADH monolayer indicate that KCl perturbs the ADH monolayer by the increment of β-structure resulting into larger unfolding and intermolecular aggregates at high salt concentration.

1. Introduction

The studies on the thin films of protein/enzyme have emerged due to their use in the chromatographic purification of a variety of drugs, peptides, antibodies, and biosensors applications.[1–7] A variety of methods have been introduced to immobilize biomaterials onto solid matrix surfaces, such as drop cast, sol−gel process, self-assembly, and Langmuir−Blodgett (LB) techniques etc.[8–13] Among these numerous techniques, the LB system is advantageous for the fabrication of monolayer and/or multilayer films with more closely packed architecture and controllable structure in the molecular level.[14]

Generally, for the preparation of protein/enzyme film by LB method, the aqueous solution of proteins/enzymes is spread very carefully on the water subphase and then the monolayer is compressed to a desired surface pressure for its successful immobilization onto appropriate substrate. This is the elementary process associated with the preparation of thin film of protein by LB technique. The main disadvantage of this process is that due to the dissolution affinity of protein/enzyme molecules into water subphase, the surface pressure and molecular area of the obtained monolayer of protein may decrease with time. As a result, one may not get actual area/molecule of the monolayer since the monolayer is not perfectly a Langmuir monolayer. As the interactions between ions and protein/enzyme in aqueous solutions play an important role, addition of some amount of salt in the subphase is used for decreasing the quantity of molecules of protein/enzyme that sink into the bulk, resulting in the configuration of more stable and organized Langmuir monolayer.[15–19] The understanding of conformational change, structural alteration and denaturation of protein/enzyme LB film transferred from electrolyte subphase are the fundamental points associated with protein/enzyme monolayer and remain not very transparent so far. Therefore, we have focused our attention to acquire some understanding about the interfacial behavior on a salt (KCl) containing subphase of an enzyme, yeast alcohol dehydrogenease (ADH), which is widely used as an alcohol sensor.[13,20] The foremost aims of this study are the conformational change, denaturation, and the surface morphology of LB film of ADH transferred from KCl containing subphase.

In this article, the interfacial surface activity of ADH was studied in absence and in presence of KCl by monitoring the surface pressure (π)-area (A) isotherm. The monolayer compressibility study was done to characterize the states of ADH monolayer and to get the information about squeezing out of ADH from different monolayers at different conditions. The conformational change of ADH in different media was studied by circular dichroism (CD) and FTIR spectroscopy. Atomic force microscopy (AFM) was employed to analyze the structural and morphological aspects of deposited ADH films at different conditions.

2. Experimental Section

2.1. Materials. The yeast alcohol dehydrogenease was purchased from Sigma Chemical Co. and used as received without further purification.

2.2. Methods. ***2.2 (A) Process of Substrate Cleaning.*** The hydrophilic glass and quartz substrates were cleaned very carefully by the process described in our earlier literature.[9]

2.2 (B) Surface Pressure−Area (π−A) Isotherm Measurement. Surface pressure−area ($\pi-A$) isotherms were recorded on a Teflon-bar-barrier type LB trough (model 2000C, Apex Instruments Co., India). The subphase was triple distilled water, deionized with a Milli-Q water purification system from Millipore, U.S.A. The pH and the resistivity of freshly prepared water were 6.8 and 18.2 MΩ cm, respectively. The surface pressure was measured using a Wilhelmy plate method with the accuracy of ± 0.1 mN/m. All experiments were conducted at an ambient temperature of 26 ± 1 °C unless otherwise mentioned.

For $\pi-A$ isotherm measurement, a known amount of aqueous solution of ADH of concentration (C_{ADH}) of 0.1 mg/mL was spread using a micro syringe on the pure water subphase on the LB trough. The spreading was done in such a manner that the surface pressure would not rise above 0.5 mN/m. Subsequently, the monolayer was slowly compressed with a compres-

* To whom correspondence should be addressed. Tel: +91-33-24734971. Fax: +91-33-24732805. E-mail: spgbt@iacs.res.in.
† Indian Association for the Cultivation of Science.
‡ Narajole Raj College.

10.1021/jp9001059 CCC: $40.75
Published on Web 03/25/2009

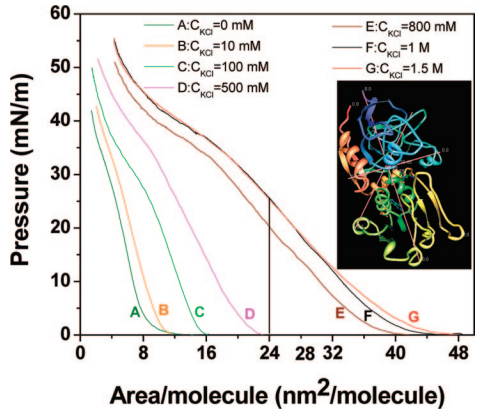

Figure 1. $\pi-A$ isotherm of ADH. Curve A is in pure water subphase. Other curves, B−G represent the isotherms of ADH at subphase containing various concentrations of KCl (C_{KCl} = 10 mM, 100 mM, 500 mM, 800 mM, 1.0 M, 1.5 M, respectively). The upper inset represents the monomeric structure of ADH. This figure is obtained from Protein data bank.

sion speed of 5 mm/min. KCl with different concentrations (C_{KCl}) was added in the subphase before $\pi-A$ isotherm measurement of ADH on electrolyte subphase.

2.2 (C) Monolayer Transfer. The monolayers were then transferred very carefully at desired surface pressure with a speed of 5 mm/min onto hydrophilic glass coverslips, silicon wafers and quartz slides, which were previously immersed in the pure and salt containing water subphases.

2.2 (D) Measurement of CD Spectra. Circular Dicroism (CD) spectra of pure aqueous solutions and KCl containing solutions of ADH and LB films of ADH lifted on quartz substrate were recorded at room temperature on JASCO J-815 CD spectrometer (Model No J-815−150S). In the solutions, the concentration of ADH was 0.01 mg/ml. The concentrations of electrolytes in ADH solutions were 1.5 M for CD spectra measurement. For CD measurement, the above-mentioned LB film of ADH was lifted on hydrophilic quartz substrate at π = 35 mN/m. Three scans were averaged to increase S/N ratio of the CD of the solution and thin films.

2.2 (E) Measurement of FTIR Spectra. FTIR spectra of LB films lifted on silicon wafers were recorded at room temperature on Magna-IR (Model No 750 spectrometer, series II), Nicollet, U.S.A. In all the cases, the data were averaged over 100 scans. The resolution of the instrument is 4 cm^{-1}.

2.2 (F) Study of Surface Morphology. The surface morphology of all films at different surface pressures was studied by an atomic force microscope (AFM, VECCO diCP-II (Model No AP-0100). The tapping mode was used in air to minimize any kind of force exerted on the ADH from the scanning tip. Thin phosphorus-doped silicon cantilever (with no coating on front side and 50 ± 10 nm aluminum coating at the back side) of resistance 1−10 Ωcm was used for scanning. The thickness of the cantilever ranges form 3.5−4.5 μm with a length of 115−135 μm as well as width of 30−40 μm. The processed images were subsequently analyzed for diameter, height and surface roughness by Proscan 1.8 image analysis 2.1. The line profiles were used to calculate surface roughness. The height profile showed the variation between highest peak and lowest valley along the line.

3. Results and Discussion

3.1. Characteristics of Pressure−Area Isotherms. The studied $\pi-A$ isotherm (trace A of Figure 1) of ADH monolayer on the surface of pure water subphase indicates that the surface pressure starts to increase at the area/molecule ≈ 13 nm^2 due to compression. As observed from this figure, the mean area/molecule estimated by extrapolating the steeply rising part of the $\pi-A$ isotherm curve to zero pressure, is ∼5 nm^2/molecule. The inset of Figure 1 shows the structure and dimension of ADH monomer obtained from protein data bank.[21] Considering the dimension of ADH monomer (6.2 nm × 4.9 nm × 3.9 nm), the estimated value of area/molecule of ADH monolayer should be around 24−30 nm^2, depending on the orientation of ADH on subphase.[21] Therefore, the value of the mean area/molecule as obtained from the isotherm is much less, than that of estimated value; indicates that most of the ADH molecules sink or dissolve into the water subphase. In this context, it is necessary to state that ADH molecules are soluble in water and thus one cannot get true area/molecule of ADH molecules into the pure water subphase. Changes in π during compression are supposed to be only due to the structural rearrangement of hydrophobic moieties of ADH molecules aligned toward the air at the air/water interface. There are several literatures on this topic.[9,15−17,22]

The $\pi-A$ isotherm of ADH shows a gaseous (G) state between the surface pressures of 0 to 1.5 mN/m where the area/molecule drops from 13 to 10 nm^2. It also shows a liquid (L) state where there is a monotonous increase of π up to ∼20 mN/m on pure water subphase. Similar nature of L state was found in case of other proteins, like ovalbumin and apolipoproteins.[9,19] Moreover, a slight bending toward left is observed between the surface pressures of 20 to 35 mN/m, though it is not prominent in the isotherm. The origin of this bending of the isotherm toward lower area/molecule at higher surface pressure is not very clear to us. However, this may be due to partial squeeze-out of the ADH (or part of the ADH) preceding the full collapse, as observed in other proteins.[9,19,23,24] The AFM images of the films, transferred at π = 35 mN/m, also supports this observation and will be discussed latter in the appropriate section.

We mentioned earlier that the addition of a certain amount of salt in the subphase might decrease the solubility of protein/enzyme molecules resulting in the formation of close packed and organized monolayer.[17,25,26] One may get a true area/molecule by using high salt concentration in the water subphase.[26] The traces B to G in Figure 1 represent the π-A isotherms at various C_{KCl} from 10 mM to 1.5 M. Results indicate that the increment of salt concentration increases the area/molecule of the ADH. The trace F represents the $\pi-A$ isotherm of ADH monolayer on the subphase containing C_{KCl} = 1.0 M, where the limiting area/molecule becomes ∼45 nm^2/ADH. Above this concentration (C_{KCl} = 1.5 M), almost overlapping isotherms are found. At the higher concentration of KCl (C_{KCl} ≥ 1.0 M), the G state occurs between the regions of area/molecule ∼48 nm^2 (at π = 0 mN/m) to ∼42 nm^2 (at π = 1 mN/m). This is clearly observed in compressibility study, discussed latter. The isotherm for C_{KCl} = 1.5 M, the L state goes up to ∼ 35 mN/m and then partial squeeze-out of the ADH (or part of the ADH) before the full collapse occurs. The observed area/molecule at the stripper region, before squeezing out of ADH from the monolayer is ∼24 nm^2, matches almost with the estimated value. Although a similar value of area/molecule at C_{KCl} = 800 mM is found in trace E, however we have not considered this as true isotherm, because above this C_{KCl} the limiting area/molecule increases. The changes of the transition region associated with the isotherms is found promi-

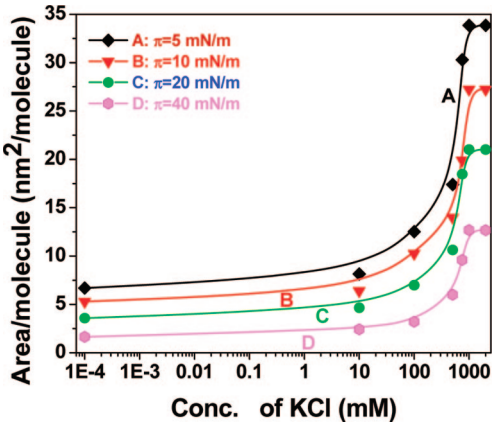

Figure 2. Area/molecule versus log (C_{KCl}) plots at different π. (A) π = 5 mN/m, (B) π = 10 mN/m, (C) π = 20 mN/m, (D) π = 40 mN/m.

nent in compressibility study, which will be discussed in the next section.

Figure 2 describes the changes in area/molecule of ADH with C_{KCl} for different fixed π. Here the traces A, B, C, and D represent the changes in area/molecule of ADH for π = 5, 10, 20, and 40 mN/m, respectively. All the traces show that there is not much change (almost constant) of area/molecule of ADH up to C_{KCl} = 10 mM. However, it is interesting to observe that there is a rapid increase of area/molecule of ADH from C_{KCl} = 0.1 M and saturation occurs at C_{KCl} = 1.0 M.

It is reported theoretically that the DLVO theory, named after Derjaguin, Landau, Verwey and Overbeek of inter particle interactions treats colloid stability in terms of a equilibrium of attractive van der Walls forces and the repulsive electrostatic forces due to the so-called double layer of counterions.[27,28] In DLVO theory, the electrostatic interaction is described using the Poisson−Boltzmann equation where the ions are treated as point charges. The DLVO theory works rather well at low salt concentrations up to 0.01 M, where electrostatic forces dominate.[27,28] In our experiment, the area/molecule of ADH is almost constant up to C_{KCl} =10 mM, which may be explained in terms of the DLVO theory of inter particle interaction. The energy barrier due the repulsive forces prevents two particles approaching one another and adhering together. However, in course of the Brownian motion of the particles, they collide with sufficient energy to overcome that barrier, the attractive force will then pull them into contact where they adhere together and the proteins/enzymes will be more soluble in the subphase. In our case, this phenomenon is probably operated in the subphase containing low concentration of KCl.

The theory looses its validity at higher salt concentration (0.1 M or higher). Ninham et al. and Bostrom et al.[29,30] have recently includes that not only electrostatic interaction but also many body ion-protein dispersion potentials, originated from polarizabilities of ions and proteins, are responsible at high salt concentration.[28,31] We believe that the sudden increment of area/molecule of ADH above C_{KCl} = 0.1 M may be due to many body ion protein dispersion potentials.

3.2. Compressibility Study. Compressibility study of Langmuir monolayer has become a useful tool to characterize the transition regions, obtained from $\pi-A$ isotherm more prominently.[32–35] The compressibility coefficient (β) is calculated by using the following equation.[32,33]

$$\beta = -\left(\frac{1}{A}\right) \cdot \left(\frac{\delta A}{\delta \pi}\right)_T \quad (1)$$

Any phase transition is reflected as a peak in the $\beta-\pi$ curve indicates the maximum compressibility (β_{max}) of monolayer, represents the greatest intermolecular cooperativeness. The asymmetry of the peak indicates that phase transition may consist of several steps.[32] The Figure 3 represents the $\beta-\pi$ curves of ADH in water and in KCl containing subphases. In case of pure water subphase (trace A in Figure 3), a broad peak is observed at higher surface pressure region between π = 24 to 32 mN/m with β_{max} =0.09 m/mN at π = 30 mN/m. This arises may be due partial squeeze-out of the protein (or part of the protein) preceding the full collapse. In case of KCl containing subphase (traces B to G in Figure 3), the position of peaks are shifted toward the higher surface pressure, indicates that squeezing out process is inhibited with dissolved salt and more pressure is required to squeeze out molecule. It is interesting to observe that the position of peak is not shifting much up to C_{KCl} = 10 mM, whereas a sudden shifting of peak position toward higher surface pressure above C_{KCl} = 0.1M. This observation is represented in the inset in Figure 3, could be explained in the same arguments in line of the DLVO theory as explained earlier in case of isotherms.

Squeezing out of ADH at higher surface pressure in case of salt containing subphase indicates the loss of rigidity of ADH molecules. The change of the peak positions in case of KCl containing subphase than pure water subphase, indicates the occurrence of some perturbation that leads to change in conformations, flexibility and unfolding of ADH molecules. A large decrement of height of β_{max} at low C_{KCl} is observed than those of at higher C_{KCl} (indicated in the inset of Figure 3) reveals that monolayer is more cooperative in low C_{KCl}.

In protein solution, there exits a hydration shell of water surrounding the protein molecule, which is different from bulk water.[36,37] The molecules of water in protein solution in general fall into following three groups.[38–40] (a) The water molecules filled inside the cavities of a protein play an important role in the process of folding and overall stability of the protein. (b) An ordered network of water molecules on the protein surface, attached through hydrogen bonds to the atoms of oxygen and nitrogen or to the polar groups of the amino acids residues. These two groups of water molecules are considered as integral parts of a protein. (c) The last group is disordered or bulk water molecules.

When the aqueous solution of ADH is introduced on to the subphase containing KCl, different interactions (electrostatic, nonelectrostatic and hydration) such as ion−ion, ion−water, water−water, protein−water, protein−ion, and protein−protein may occur.[40] The above interactions determine finally whether the protein is a macro-cation or a macro-anion.[40] Since, the small ions are strongly hydrated; it would be difficult to remove a water molecule from a small hydrated ion. At low salt concentration below 10 mM, the magnitude of above distant dependent interactions is negligible, as a result no appreciable change of area/molecule and compressibility occur at low salt concentration. On the other hand, at high salt concentration above 10 mM, the large electrostatic interaction and hydration forces drive the nonelectrostatic and depressive interactions, which in effect increase the dissolubility of the protein in the subphase, as a result a sharp increase of area/molecule and compressibility occur. When hydrated ions approach a hydrated ADH molecule, the network of water around the ions and the protein is disturbed leading to a hydrated ion-protein entity.

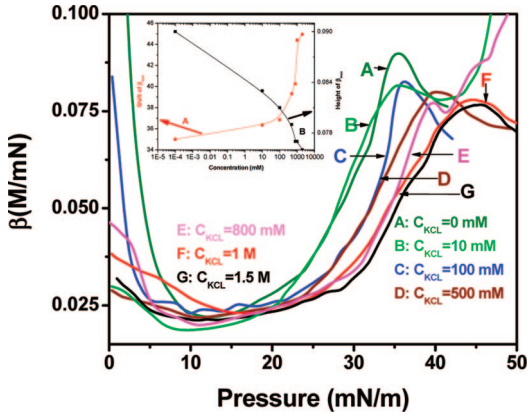

Figure 3. $\beta-\pi$ plots of ADH. Curve A is for pure water subphase. Curves B−G represent similar plots at subphase containing various concentrations of KCl (C_{KCl} = 10 mM, 100 mM, 500 mM, 800 mM, 1.0 M, 1.5 M, respectively).(Inset) Plot of shift of β_{max} vs C_{KCl} (A) and height of β_{max} vs C_{KCl} (B).

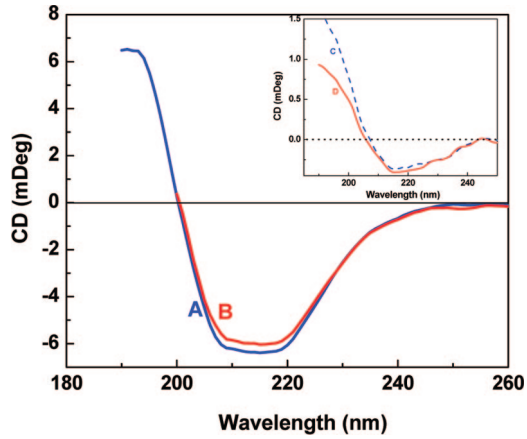

Figure 4. CD spectra of ADH. (A) In pure aqueous solution. (B) ADH in KCl containing solution. (Inset, C) LB film lifted from pure water subphase. (D) LB film lifted from KCl containing water subphase.

When several such entities approach each other, a cascading effect arises leading to assemblies of hydrated ions plus protein. Such large size assemblies possibly account for distorted or partially unfolding of protein.[40]

3.4. CD Spectroscopy Study. The far-ultraviolet region (185−250 nm) of CD spectroscopy is used to study the change in conformation of ADH. A comparative study among the CD spectra of ADH in water solution, in aqueous solution of KCl and in LB films of ADH is made. When a polypeptide chain existed in the α-helical conformation, two negative bands at ∼209 nm and ∼222 nm and a positive band at ∼190 nm[41,42] are observed. The 209 nm band corresponds to $\pi-\pi^*$ transition of α-helix whereas the 222 nm band corresponds to $\pi-\pi^*$ transition for both α-helix and random coil.[19] On the other hand, for the existence of β-sheet, a positive and a negative band appeared at 190 and 215 nm respectively.[41,42]

Figure 4 shows the far-UV CD spectra of ADH in different conditions. The observed spectrum of ADH in aqueous solution (trace A) has broad negative bands around at ∼209 and 220 nm, almost similar as reported by earlier literature, confirms a α-helical structure.[43] We also observe a positive band at ∼190 nm. It is reported that the secondary structure of ADH at neutral pH consist of ∼32% α-helix.[43,44] The secondary structure of ADH is well maintained when ADH is dispersed in high concentrated KCl (1.5 M) solution (trace B). A similar result was found in case of apolipoproteins in high concentrated KCl (3.5 M) solution.[19]

The inset of Figure 4 shows the CD spectrum of ADH in LB film from pure water subphase at π = 30 mN/m (trace C) and KCl containing subphase at π = 35 mN/m (trace D). In both the spectra, we observe a prominent negative band at ∼215 nm and a positive band at ∼190 nm implies prominent increment of β-structure resulting into unfolding and intermolecular aggregates of ADH. Study of AFM images, discussed later, also confirms this observation. Similar unfolding of protein at air/water interface reported in earlier literature.[45] The ellipticity of the negative band at 215 nm is more in case of the spectra of the LB film lifted from KCl containing subphase than that of pure water subphase. This implies that the increment of β-structure of ADH monolayer is greater in salt containing subphase than in pure water subphase. Thus, a greater unfolding of ADH is observed for salt containing subphase. It is interesting to note that the perturbing effect of salts on ADH monolayer is detectable in the CD spectra whereas it is undetectable in salt containing ADH solutions.

As it is very difficult to calculate the actual amount of α and β-components of protein in case of thin film, we have tried to interpret the CD spectrum of ultrathin film using the peak position and ellipticity. In the next section, we will discuss and try to estimate the different components of secondary structure of ADH in different thin films by FTIR spectroscopy.

3.5. FTIR Study. The panels A and B of Figure 5 represent the FTIR spectra of thin LB film of ADH lifted from pure water and 1.5 M KCl containing subphase at π = 35 mN/m respectively. Unfolding, intra- and intermolecular associations of ADH were studied by monitoring the peak positions and widths of two amide bands within a fixed range.[46] Both the spectra (panels A and B) consist of two broad peaks from 1500 to 1600 cm^{-1} and from 1600 to 1700 cm^{-1}. The spectrum from 1600 to 1700 cm^{-1} is the vibration band of amide-I, mainly resulted from carbonyl stretching vibrations of the peptide backbone, sensitive to the peptide secondary structure like α-helices, β-sheets or β-turns. The vibrational frequency of each C═O bond depends on the strength of hydrogen bond and the interactions between the amide units, both of them are influenced by the secondary structure.[46,47] The peak from 1500 to 1600 cm^{-1} can be ascribed to the vibration band of amide-II resulted from a combination of N−H in-plane bending and C−N stretching vibrations of peptide groups.[46,47] The vibrational energies of the carboxyl group depend on the different conformations of the protein, such as α-helix, β-sheet, β-turns, intra- and intermolecular aggregates. The determination and the assignment of the spectral components of the amide-I band can then provide information on the secondary structure of protein.[46,48] The deconvolution of the normalized amide-I band is useful to study the conformations of the protein/enzyme. Generally, Lorentzian, Gaussian and/or a mixture of these functions are used to describe the components.[49] The deconvolution using Lorentzian function would be more appropriate at low temperature. However, at elevated temperature, different types of broadening, such as phonon broadening may come into play and perturbs the line shape. We think the use of Gaussian function would be more appropriate, as we are working at room temperature. A multiple peak fitting technique with Gaussian profile using Micro Cal Origin 7.5 was employed to fit normalized amide-I band to study the conformations of ADH. This multicomponent fitting of the profile allows one to identify different components and in particular to determine the corresponding peak frequencies. The percentage area of the deconvoluted peaks gives the relative amount of components. It is worth noting that in all the spectra considered in the present

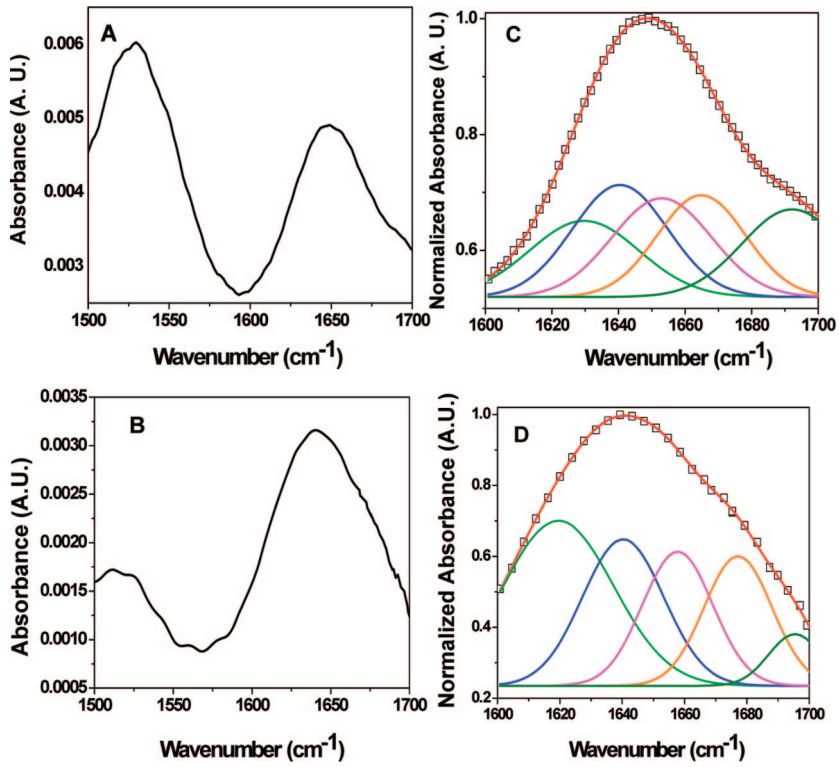

Figure 5. FTIR spectra of ADH LB film. (A) Pure water. (B) KCl containing subphase. (C) Deconvolution of amide I band of A. (D) Deconvolution of amide I band of B.

work, the maximum number of the components (N), which can be identified in the deconvoluted amide-I band, is 5 to have a meaningful fitting. Neither use of lesser number of peaks, the fitting gives satisfactory result nor more number of peaks improves R^2 values nor the deconvoluted peaks have definitive positions. We have targeted different peak values for different components to fit the band. The targeting frequencies for β-sheet mode (β-component) and for α-helix mode (α-component) are 1638 cm^{-1} and 1654 cm^{-1} respectively. Since the secondary structures are stabilized by hydrogen bonds between amide C═O and N−H groups, the position of the components depends on the patterns and the strength of the hydrogen bonds. For stronger hydrogen bonding, the vibration is observed at higher wavenumber. The β- sheet structures have the strongest hydrogen bonds, exhibit an amide I maximum at much lower frequency than α-helices.[47] The 1618 and 1683 cm^{-1} bands are assigned to inter (A_1 component) and intra (A_2 component) molecular aggregates respectively. In case of aggregates, the hydrogen bonds formed between C═O and N−H groups of any polypeptides strands with which they come in contact. The consequence is that many hydrogen bonds are formed between polypeptide chains in neighboring protein molecule, forming an aggregate stabilized by very strong intermolecular hydrogen bonds.[47]The 1666 cm^{-1} component can be ascribed to the vibration modes originated by β-turns in the structures (T-component).[46,47,50–55]

The panels C and D of Figure 5 represent the fitting curves of normalized amide-I peak of LB thin film of ADH lifted from pure water subphase and from KCl containing subphase respectively. The fitted results are reported in Table 1. For all the fittings the square of the correlation coefficient, R^2 is found to be 0.999. The summary of the fitted result is indicated in Figure 6 by bar diagram. The β/α ratio for different films are presented in the inset of Figure 6.

Figure 6 shows that the LB film of ADH lifted from pure water subphase is composed of high amount of β-component (22.93%) and of small amount of α-component (20.99%). Since the β/α ratio (1.092) is greater than unity, some α helix may be converted into β sheet. In addition, large values of A_1 (17.96%) and A_2 (18.88%) indicate that there are mostly larger intermolecular aggregates. The LB thin film of ADH lifted from KCl containing subphase is also composed of relatively high amount of β-component (23.32%) and of small amount of α-component (18.45%). The β/α ratio (1.25) is greater than LB film of ADH lifted from pure water subphase. Thus, more amount of α helix is converted into β sheet in case of KCl containing subphase than pure water subphase. Moreover, large value of A_1 (35.65%) in contrast to low value of A_2 (5.35%) indicates that there are mostly larger intermolecular aggregates with greater unfolding of ADH.

TABLE 1: Fitting Parameters Using Multipeak Fitting of Amide-I Band for ADH Thin Film[a]

	area (%)		position (cm^{-1})		fwhm (cm^{-1})	
conformers	A	B	A	B	A	B
A_1	17.96	35.65	1629.7	1619.5	33.13	35.41
β	22.93	23.32	1640.5	1640.2	28.68	26.07
α	20.99	18.45	1653.1	1657.7	29.88	22.55
T	19.24	17.23	1665.1	1677.0	26.56	21.78
A_2	18.88	5.35	1692.1	1695.2	30.23	18.80

[a] A represents LB film of ADH lifted from pure water subphase, B represents LB film of ADH lifted from KCl subphase. Area (%) = 100 represents the total area under curve. fwhm represents full width at half-maximum of a peak.

3.5. AFM Study. To correlate the structural changes as inferred from the CD spectra of ADH with actual changes in the morphologies of the structures, the AFM studies of the LB films of ADH were performed.

Figure 7 shows the AFM image of ADH film lifted at π = 5 mN/m from pure water subphase, taken over an area of 800 nm × 800 nm. Throughout the film, we observe globular

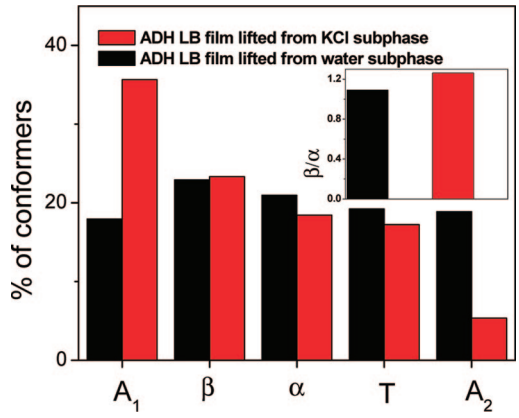

Figure 6. Comparative Bar-Diagram of different structural parameters of ADH in presence and absence of KCl (values are shown in Table 1).

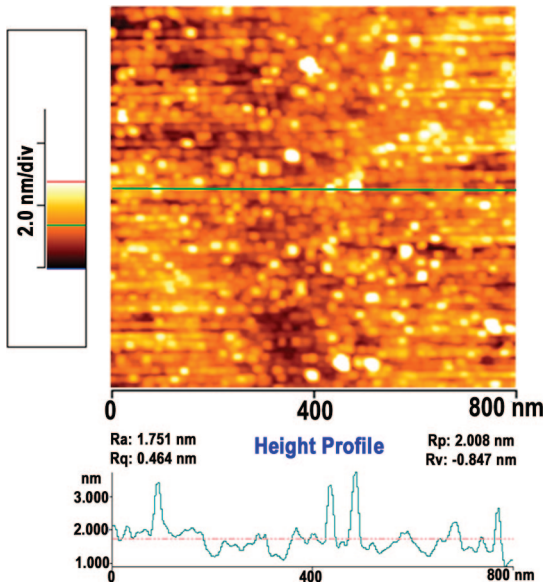

Figure 7. AFM image of LB film of ADH in nanometer scale with height profile, lifted from pure water subphase at $\pi = 5$ mN/m.

domains. The dimensions of these domains are in the range of 20−30 nm in diameter. Thus, the observed globular domains may be the aggregates of four to eight units of ADH molecules. This observation also supports the increment of β-structure with unfolding of ADH, which may eventually form the intermolecular aggregates as concluded from FTIR study.

Figure 8 shows the AFM image of ADH monolayer lifted at $\pi = 35$ mN/m from pure water subphase, taken over an area of 250 nm × 250 nm. Comparing this film with film of Figure 7, one can see that the surface morphology is different. From the height profile we observed that this film consist of two layers. Here we observed that squeezed out aggregates of ADH. A large amount of nano aggregates are scattered on the upper portion of the film. These nano aggregates are the direct evidence of squeezing out of ADH at higher surface pressure. This squeezed out molecules are not globular, may be due to greater unfolding of ADH molecules those were in completely in the air phase. Therefore, the AFM image supports the observations and the arguments of the $\pi-A$ isotherm and $\beta-\pi$ curve studies. Careful observation of the image shows that the squeezing out aggregates are more branching and appear too linked together in a fractal network.

Earlier we have found that the squeezed out region of ADH changes by using KCl in subphase. We have studied the surface

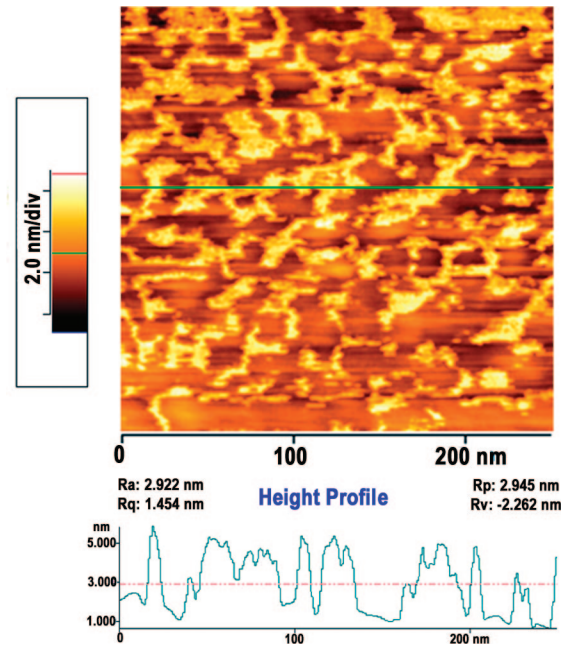

Figure 8. AFM image of LB film of ADH in nanometer scale with height profile, lifted from pure water subphase at $\pi = 35$ mN/m.

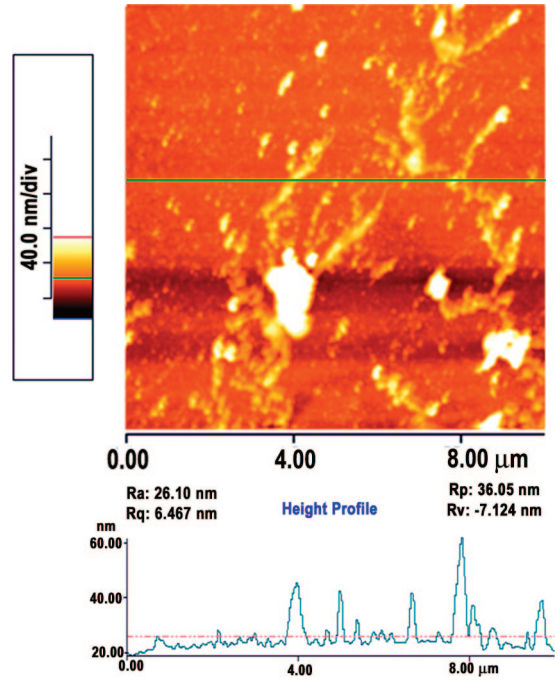

Figure 9. AFM image of LB film of ADH in micrometer scale with height profile lifted from KCl containing subphase at $\pi = 35$ mN/m.

morphology of the monolayer after transition region at higher surface pressure. Figure 9 shows the surface morphology of the monolayer lifted from 1.5 M salt containing subphase at $\pi = 35$ mN/m taken over an area 10 μm × 10 μm. Here we have found different fibrillar type aggregated structure. These fibrils may be the amyloidal fibrils of ADH.[33] In pure water, we did not found this type of aggregates. On closer look, we also feel that the aggregated structure may be fractal in nature.

The cause behind of this type of fractal/fibrillar aggregates formation is unknown to us. It is reported that the increment of β-structure is necessary for the formation of amyloid fibrils.[56–58] The CD and FTIR study supports that in KCl containing

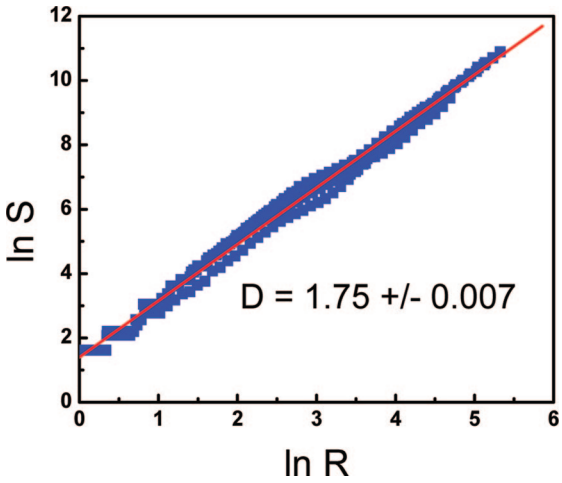

Figure 10. ln (S) vs ln (R) plot for Figure 8. The least-squares method is used for straight-line fitting. The error in slope determination is coming from line fitting.

subphase the increment of β-structure with unfolding of ADH and the formation of intermolecular aggregates (A_1) are larger than pure water subphase. The increment of intermolecular aggregates of ADH molecules and the interaction among themselves at higher surface pressure may be the feasible cause for the formation of amyloidal micro fibrils. In higher magnification, we find similar structure of monolayer like. This figure is not included in the text.

We have tried to analyze probable fractal structures. The fractal dimension has been calculated by using the radial mass distribution method. The Hausdorff dimension, D, is related as $S \propto R^D$, where, S is the area covered by each structure, R is the average distance from the center of mass of a structure to its perimeter. Accordingly, slope of a linear fit of ln (S) vs ln (R) should yield the fractal dimension of an assembly of nano structure. Figure 10 shows such a plot after analyzing the AFM image of ADH monolayer lifted at surface pressure = 35 mN/m from pure water subphase (Figure 8). Data are taken in different region of the AFM image and fitted to straight line by least-squares method. The value of fractal dimension (D) is 1.75 $\pm$ 0.0.007. Similar analyses yields $D = 1.95 \pm 0.0.005$ for the AFM image of ADH monolayer lifted at surface pressure = 35 mN/m from 1.5 M salted subphase (Figure 9). Higher value of fractal dimension ($D \approx 1.95$) in the salty subphase indicates that aggregated structures are mostly lumpy in nature. Whereas in pure water at high-pressure, nano structured aggregates are more fractal in nature. This type of growth may be initiated due to intrinsic unfolding of protein followed by β sheet formation at air water interface.

4. Conclusion

In this work, the interfacial surface activity of ADH in presence and in absence of KCl is studied by monitoring the surface pressure (π)-area (A) isotherm measurement and in situ detail compressibility study. The unfolding of ADH in different media is studied by circular dichroism (CD) and FTIR spectroscopy. CD and FTIR study shows that salt perturb the ADH monolayer. A larger increment of β-structure together with larger unfolding and intermolecular aggregates of ADH molecules is expected by using salt in subphase. The perturbing effect of salts on ADH monolayer is detected after study the CD spectra of ADH monolayer lifted from salt containing subphases. It was undetectable by comparing the CD spectra of pure and salt containing ADH solutions. AFM study reveals that, at higher surface pressure ADH is squeezed out from the monolayer. In case of salt containing subphase micro amyloidal fibrils are observed. Aggregated structures are more branching and appear too linked together in a fractal network.

Acknowledgment. We thank DST, Government of India (Project No.-SR/S2/CMP-0051/2006) for partial financial support. Mrityunjoy Mahato also thanks CSIR, Government of India for providing the CSIR-NET fellowship.

References and Notes

(1) Girard-Egrot, A.; Godoy, P. S.; Blum, L. *J. Adv. Colloid Interface Sci.* **2005**, *116*, 205.
(2) Beigi, F.; Lundahl, P. *J. Chromatogr. A* **1999**, *852*, 313.
(3) Okahata, Y.; Tsuruta, T.; Ijiro, K.; Ariga, K. *Langmuir* **1988**, *4*, 1373.
(4) Ramsden, J. J. *Biosens. Bioelectron.* **1998**, *13*, 593.
(5) Hou, S.; Wang, J.; Martin, C. R. *Nano Lett.* **2005**, *5*, 231.
(6) Siwy, Z.; Trofin, L.; Kohli, P.; Baker, L. A.; Trautmann, C.; Martin, C. R. *J. Am. Chem. Soc.* **2005**, *127*, 5000.
(7) Léger, C.; Bertrand, P. *Chem. Rev.* **2008**, *108*, 2379.
(8) Lee, J. B.; Kim, D.; Choi, J.; Koo, K. *Colloids Surf. B: Biointerfaces* **2005**, *41*, 163.
(9) Kamilya, T.; Pal, P.; Talapatra, G. B. *J. Phys. Chem. B* **2007**, *111*, 1199.
(10) Kamilya, T.; Pal, P.; Mahato, M.; Talapatra, G. B. *J. Nanosci. Nanotech.* in press.
(11) Kamilya, T.; Pal, P.; Mahato, M.; Talapatra, G. B. *Mater. Sci. Eng. C* http://dx.doi.org/10.1016/j.msec. 2008.12.003.
(12) Ariga, K.; Hill, J. P.; Lee, M. V.; Vinu, A.; Charvet, R.; Acharya, S. *Sci. Technol. Adv. Mater* **2008**, *9*, 014109.
(13) Pal, P.; Nandi, D.; Misra, T. N. *Thin Solid Films* **1994**, *239*, 138.
(14) Rosilio, V.; Boissonnade, M. M.; Zhang, J.; Jiang, L.; Baszkin, A. *Langmuir* **1997**, *13*, 4669.
(15) Ahluwalia, A.; De Rossi, D.; Shirone, *J. Biosens. Bioelec.* **1991**, *6*, 133.
(16) Turko, I.; Yurkevich, I.; Chashchin, V. *Thin Solid Films* **1991**, *205*, 113.
(17) Dziri, L.; Puppala, K.; Leblenc, R. M. *J. Colloid Interface Sci.* **1997**, *194*, 37.
(18) MacRitchie, F. *J. Colloid Interface Sci.* **1985**, *105*, 119.
(19) Bolanos-Garcia, V. M.; Ramos, S.; Castillo, R.; Xicohtencatl-Cortes, J.; Mas-Oliva, J. *J. Phys. Chem. B* **2001**, *105*, 5757.
(20) Liu, S.; Cai, C. *J. Electroana. Chem.* **2007**, *602*, 103.
(21) Protein Data Bank (Yeast alcohol dehydrogenease).
(22) Chen, X.; Yang, T.; Kataoka, S.; Cremer, P. S. *J. Am. Chem. Soc.* **2007**, *129*, 12272.
(23) Kamilya, T.; Pal, P.; Talapatra, G. B. *Colloids Surf. B: Biointerfaces* **2007**, *58*, 137.
(24) Kamilya, T.; Pal, P.; Talapatra, G. B. *J. Colloid Interface Sci.* **2007**, *315*, 464.
(25) Chudinova, G. K.; Pokrovskaya, O. N.; Savitskii, A. P. *Russ. Chem. Bull.* **1995**, *44*, 1958.
(26) Xicohtencatl-Cortes, J.; Mas-Oliva, J.; Castillo, R. *J. Phys. Chem. B* **2004**, *108*, 7307.
(27) Israelachvili, J. *Intermolecular and surface forces*, II ed.; Academic Press Inc.: New York, 991.
(28) Zhang, Y.; Cremer, P. S. *Curr. Opin. Chem. Biol.* **2006**, *10*, 658.
(29) Ninham, B. W.; Yaminsky, V. *Langmuir* **1997**, *13*, 2097.
(30) Bostrom, M.; Williams, D. R. M.; Ninham, B. W. *Biophys. J.* **2003**, *85*, 686.
(31) Moreira, L. A.; Bostrom, M.; Ninham, B. W.; Biscaia, E. C. F.; Tavares, W. *Colloid Surf., A* **2006**, *457*, 282.
(32) Yu, Z. W.; Jin, J.; Cao, Y. *Langmuir* **2002**, *18*, 4530.
(33) Ihalainen, P.; Peltonen, J. *Langmuir* **2003**, *19*, 2226.
(34) Yin, F.; Shin, H.; Kwon, Y. *Thin Solid Films* **2006**, *499*, 1.
(35) Wan, K.; Chovelon, J.; Jaffreziic-Renault, M. N. *Talanta* **2000**, *52*, 663.
(36) Chalikian, T. V.; Totrov, M.; Abagyn, R.; Breslauer, K. J. *J. Mol. Biol.* **1996**, *260*, 588.
(37) Steinbach, P. J.; Brooks, B. R. *Proc. Natl. Acad. Sci. U.S.A.* **1993**, *90*, 9135.
(38) Szoszkiewicz, R.; Kulik, A. J.; Gremaud, G.; Lekka, M. *Appl. Phys. Lett.* **2005**, *86*, 123901.
(39) Johari, G. P.; Sartor, G. *J. Chem. Soc., Faraday Trans.* **1996**, *92*, 4521.
(40) Lakshmanan, M.; Dhathathreyan, A.; Miller, R. *Colloid Surf., A* **2008**, *324*, 194.
(41) Li, J.; Du, Y.; Boullanger, P.; Jiang, L. *Thin Solid Films* **1999**, *352*, 213.

(42) Adler, A. J. In *Methods in Enzymology*, Hirs, C. H. W.; Timasheff, N. S., Eds.; Academic Press, New York, 1973, pp 675.
(43) Shimizu, A.; Yamada, Y.; Mizuta, T.; Haseba, T.; Sugai, S. *J. Mol. Liquids* **2004**, *109*, 45.
(44) Greenfield, N.; Fasman, G. D. *Biochemistry* **1969**, *8*, 4108.
(45) Tronin, A.; Dubrovsky, T.; Dubrovskaya, S.; Radicchi, G.; Nicoloni, C. *Langmuir* **1996**, *12*, 3272.
(46) Carbonaro, M.; Maselli, P.; Dore, P.; Nucara, A. *Food Chem.* **2008**, *108*, 361.
(47) Jackson, M.; Mantsch, H. H. Protein ligand interactions studied by FTIR spectroscopy: methodological aspects. In *Protein Ligand Interactions: structure and spectroscopy*, Harding, S. E., Chowdhry, B. Z., Eds.; Oxford University Press: New York, 2001; pp 240–258.
(48) Jackson, M.; Mantsch, H. H. *Critical Rev. Biochem. Mol. Biol.* **1995**, *30*, 95.
(49) *Selected applications of modern FT-IR techniques*; Nishikida, K., Nishio, E., Hannah, R. W., Eds; Gordon and Breach publishers: Tokyo, 1995, p 268.
(50) Bhattacharjee, C.; Saha, S.; Biswas, A.; Kundu, M.; Ghosh, L.; Das, K. P. *Protein J.* **2005**, *24*, 27.
(51) Meng, G. T.; Ma, C. Y. *Int. Journal Biol. Macromol.* **2001**, *29*, 287.
(52) Bandekar, J. *Biochem. Biophys. Acta* **1992**, *1120*, 123.
(53) Murayama, K.; Tomida, M. *Biochemistry* **2004**, *43*, 11526.
(54) Barth, A. *Biochim. Biophys. Acta* **2007**, *1767*, 1073.
(55) Jackson, M.; Mantsch, H. H. *Can. J. Chem.* **1991**, *69*, 1639.
(56) Ball, A.; Jones, R. A. L. *Langmuir* **1995**, *11*, 3542.
(57) Adams, S.; Higgins, A. M.; Jones, R. A. L. *Langmuir* **2002**, *18*, 4854.
(58) Sharp, J. S.; Forrest, J. A.; Jones, R. A. L. *Biochemistry* **2002**, *41*, 15810.

JP9001059